The American Journal of Pathology, Vol. 185, No. 1, January 2015

ELSEVIER

The American Journal of
PATHOLOGY
ajp.amjpathol.org

CELL INJURY, REPAIR, AGING, AND APOPTOSIS

# Global Deletion of *Ankrd1* Results in a Wound-Healing Phenotype Associated with Dermal Fibroblast Dysfunction

Susan E. Samaras,* Karinna Almodóvar-García,* Nanjun Wu,* Fang Yu,* and Jeffrey M. Davidson*†

*From the Department of Pathology, Microbiology, and Immunology,* Vanderbilt University School of Medicine, Nashville; and the Research Service,† Veterans Affairs Tennessee Valley Healthcare System, Nashville, Tennessee*

Accepted for publication September 19, 2014.

Address correspondence to Jeffrey M. Davidson, Ph.D., Department of Pathology, Microbiology, and Immunology, Vanderbilt University School of Medicine, 1161 21 St Ave S, C-3321 Medical Center North, Nashville, TN 37232. E-mail: jeff.davidson@vanderbilt.edu.

The expression of ankyrin repeat domain protein 1 (*Ankrd1*), a transcriptional cofactor and sarcomeric component, is strongly elevated by wounding and tissue injury. We developed a conditional *Ankrd1*$^{fl/fl}$ mouse, performed global deletion with Sox2-*cre*, and assessed the role of this protein in cutaneous wound healing. Although global deletion of *Ankrd1* did not affect mouse viability or development, *Ankrd1*$^{-/-}$ mice had at least two significant wound-healing phenotypes: extensive necrosis of ischemic skin flaps, which was reversed by adenoviral expression of ANKRD1, and delayed excisional wound closure, which was characterized by decreased contraction and reduced granulation tissue thickness. Skin fibroblasts isolated from *Ankrd1*$^{-/-}$ mice did not spread or migrate on collagen- or fibronectin-coated surfaces as efficiently as fibroblasts isolated from *Ankrd1*$^{fl/fl}$ mice. More important, *Ankrd1*$^{-/-}$ fibroblasts failed to contract three-dimensional floating collagen gels. Reconstitution of ANKRD1 by adenoviral infection stimulated both collagen gel contraction and actin fiber organization. These *in vitro* data were consistent with *in vivo* wound closure studies, and suggest that ANKRD1 is important for the proper interaction of fibroblasts with a compliant collagenous matrix both *in vitro* and *in vivo*. *(Am J Pathol 2015, 185: 96–109; http://dx.doi.org/10.1016/j.ajpath.2014.09.018)*

As part of a gene expression profiling program to identify genes altered after dermal wounding in mice, we reported that ankyrin repeat domain protein 1 (*Ankrd1*; alias cardiac ankyrin repeat protein) mRNA and protein levels were highly induced and remained elevated during the healing process.[1] Cells of the epidermis and dermis that showed induced expression included vascular endothelial cells, cells of the hair follicle bulb, the panniculus carnosus, keratinocytes, monocytes, and fibroblasts, indicating increased ANKRD1 may be a generalized stress response in many cell types of the skin. Overexpression of ANKRD1, a member of the muscle ankyrin repeat protein (MARP) family, which includes *Ankrd2* and *Ankrd23*,[2] also improved many aspects of wound healing in several animal models.[1]

The dynamics of MARP gene expression during both normal muscle development and function and those seen under pathological stress conditions in muscle and many other tissues[3–5] suggested that disruptions in normal MARP function could have dire consequences to the organism. However, a recent report observed that deletions of the MARP family members, both individually and in combination, produced a subtle phenotype.[6] On the basis of the altered skeletal muscle response to eccentric contraction, the authors suggested that the MARPs are not essential for development or basal function of skeletal muscle, but that they play a role in mechanical behavior and stability of muscle after exercise. It was also concluded that the three MARP proteins are structurally and

Supported by National Institute of Diabetes and Digestive and Kidney Diseases grant DK065656-08 (J.M.D.), National Institute of General Medical Sciences fellowship GM101947-02 (K.A-G.), National Institute of Arthritis and Skin and Musculoskeletal Diseases grant AR056138 (J.M.D.), and the Department of Veterans Affairs. The Vanderbilt Transgenic Mouse/Embryonic Stem Cell Shared Resource is supported in part by the Center for Stem Cell Biology, a Cancer Center Support grant CA68485, and the Vanderbilt Diabetes Research and Training Center grant DK20593.

S.E.S. and K.A.-G. contributed equally to this work.

Disclosures: None declared.

Current address of N.W., Lab Corporation, Nashville, TN.


http://dx.doi.org/10.1016/j.ajpath.2014.09.018

functionally redundant, because it required deletion of all three genes to see a significant effect. A recent study with the same strains further concluded that the MARPs were not involved in the response to cardiac pressure overload.[7]

We developed a conditional *Ankrd1*$^{fl/fl}$ mouse with the ultimate goal of determining the role of ANKRD1 in various cell types. As an initial approach, we generated a global deletion for the purpose of studying ANKRD1 function in all cell types involved in wound healing. We now report that deletion of *Ankrd1* results in a viable mouse with significant wound-healing phenotypes that are not compensated by intact *Ankrd2* or *Ankrd23*. Results of cell culture studies suggest that part of this phenotype results from dysfunctional cell-matrix interaction in fibroblasts.

## Materials and Methods

### Recombination of *Ankrd1* Conditional KO Mice

We designed a targeting vector to delete the mouse *Ankrd1* gene basal promoter and protein-coding exons 1 and 2 (1.87 kb) when targeted mice were crossed with *cre*-recombinase–expressing mice (Figure 1A). The targeting vector was constructed using 15 kb of *Ankrd1* sequence that was retrieved from strain 129S7/SvEvBrd-Hptrb-m2 mouse bacterial artificial chromosome (BAC) library (bMQ-382E2; BACPAC Resource Center, Children's Hospital Oakland Research Institute, Oakland, CA).[8] Two *cre*-recombinase recognition sequences (loxP) were introduced into the 15-kb BAC sequence: the first loxP was located approximately 7 kb upstream of the 5′ end, and the second loxP was inserted into intron 2 approximately 6 kb upstream from the 3′ end (Figure 1A). A neomycin gene cassette flanked by *flp*-recombinase recognition (frt) sites was inserted 5′ of the second loxP site. Herpes simplex virus–thymidine kinase was also included as a negative selection marker. Internal EcoRV and SmaI sites were introduced into this 15-kb BAC DNA for confirmation of the targeted allele (Figure 1B). Embryonic stem cells (129S6) were electroporated with the linearized targeting vector in the Vanderbilt Transgenic/Embryonic Stem Cell Core (Nashville, TN), and isolated colonies were screened by Southern blot analysis. Positive clones were injected into C57Bl/6J blastocysts. Resulting male pups that were $\geq$70% chimeric were tested for germ-line transmission by breeding to C57Bl/6J females. The neomycin cassette was removed by breeding hemizygous (*Ankrd1*$^{wt/fl}$) mice to actin promoter-driven, *eflp*-recombinase C57Bl/6J mice.

Hemizygous (*Ankrd1*$^{wt/fl}$) mice with the neomycin cassette deleted were bred to homozygosity [*Ankrd1*$^{fl/fl}$; flanked by loxP (FLOX)], followed by breeding to *Sox2* promoter-driven *cre*-recombinase C57Bl/6J mice. Because the *Sox2* promoter is expressed in the oocyte,[9] all offspring acquired a recombined allele, even when the Sox2 *cre*-recombinase transgene did not segregate to the pup. Mice with deletion of one *Ankrd1* allele [*Ankrd1*$^{wt/-}$; wild type (WT/−)] were crossbred to produce homozygous [*Ankrd1*$^{-/-}$; knockout (KO)] mice. Mice lacking the Sox2-*cre* recombinase and *eflp*-recombinase transgenes were selectively used for breeding to eliminate the transgenes from the KO background. Initial phenotyping studies used mixed-breed C57Bl/6J/129S6 FLOX, *WT/*−, and KO mice. Mice were further backcrossed to C57Bl/6J to generate a pure inbred strain. The mice used for the excisional wound studies had been backcrossed for eight generations.

### Organ Weight Determination

Adult FLOX, *WT/*−, and KO mice were weighed and euthanized. The spleen, three lobes of the liver, one kidney, brain, cardiac ventricles, and the gastrocnemius muscle (skeletal muscle) were dissected and weighed. Organ/body weight ratios were calculated. Differences among the three genotypes were tested for significance using Graphpad Prism version 5.03 (GraphPad Software, Inc., La Jolla, CA) and two-way analysis of variance, with significance set at $P < 0.05$.

### Histopathological Evaluation of KO and FLOX Mice

Samples of tissue from all major organ systems of young (5 to 6 months old) and aged (>1 year) adult male and female *Ankrd1*-null mice and FLOX age-matched controls were collected, fixed overnight in formalin, processed routinely, divided into sections (5 μm thick), and stained with hematoxylin and eosin. The specimens underwent thorough gross and microscopic evaluation of all organ systems by a veterinary pathologist in the Division of Comparative Pathology, Department of Pathology, Microbiology, and Immunology, Vanderbilt University School of Medicine (Nashville, TN). No abnormalities were found.

### Surgical Wounding Models

Studies were performed in the Association for Assessment and Accreditation of Laboratory Animal Care International–approved facilities of Vanderbilt University, under approval of the Institutional Animal Care and Use Committee at Vanderbilt University School of Medicine. FLOX (control) and KO male mice (aged 15 to 20 weeks; $n = 8$, each genotype) in a mixed background and in eighth-generation C57Bl/6J background received two 6-mm, full-thickness excisional wounds on the dorsum. Wounds were photographed with a Canon PC1234 camera (Canon USA, Lake Success, NY). Wound areas were determined using ImageJ software version 1.48 (NIH, Bethesda, MD) and expressed as percentage of initial wound size. At completion of the experiment, mice were euthanized, and the complete wounds, including 2 mm of the wound margin, were harvested and prepared for histological analysis.

Large excisional wounds were used to follow wound closure rates in 15 C57BL/6 and 10 KO age-matched female mice weighing 19 to 22 g. Under isoflurane anesthesia, the dorsal surface was shaved with electric clippers, cleaned successively with betadine and 70% isopropanol (3×), and then incised with a scalpel to produce a 15 × 15-mm, full-thickness

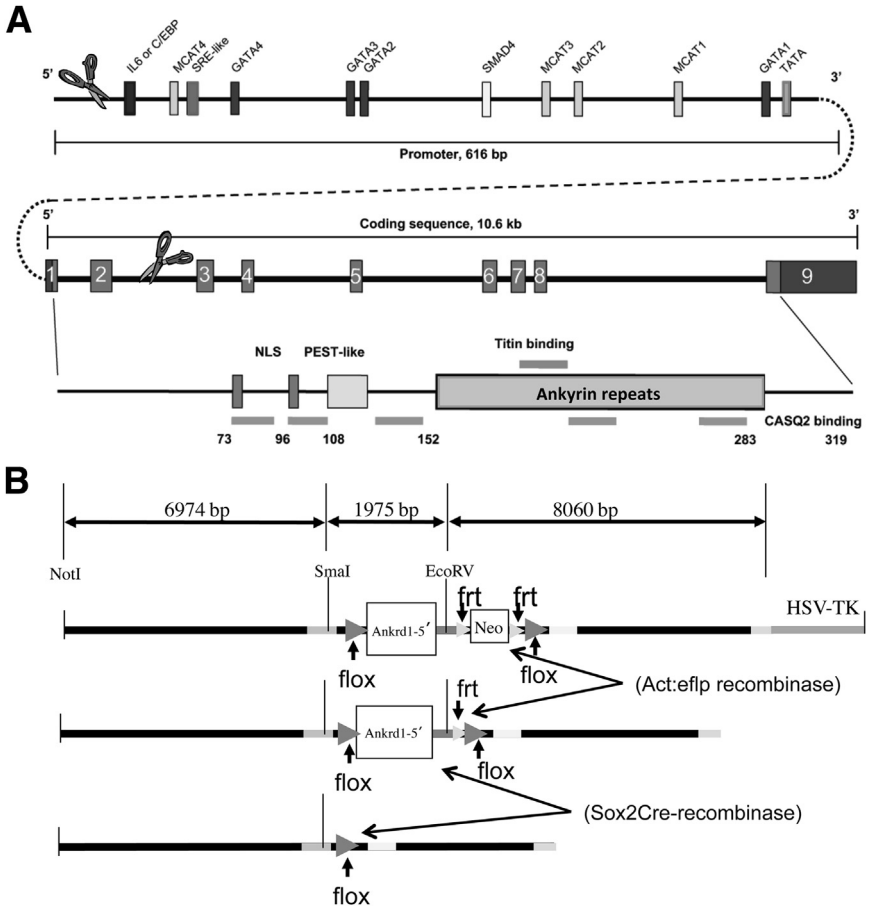


**Figure 1** Strategy for conditional deletion of murine *Ankrd1*. **A:** Graphic representation of *Ankrd1* gene structure shows the 600-bp proximal promoter with known transcription factor binding sites and the structural gene. All nine exons of the structural gene encode for some portion of the protein. Protein-encoding regions in all nine exons are shown in gray, with the domain organization shown below. Scissors indicate the region removed by *cre*-recombinase. Adapted from Samaras et al[5] and modified with permission from Nature Publishing Group. **B:** *Cre*-recombinase recognition sequences (loxP; flox) were inserted 600 bp upstream of the transcription start site and in intron 2 of the *Ankrd1* gene, which was included in a 15-kb restriction fragment from a 129S6 mouse-derived BAC clone. A neomycin resistance cassette, flanked by *eflp*-recombinase recognition sequences (frt), was inserted into intron 2 just 5′ of the downstream flox site. The neomycin resistance cassette was removed by breeding targeted mice with mice expressing actin promoter-driven *eflp*-recombinase. Subsequent breeding to mice expressing *Sox2* promoter-driven *cre*-recombinase produced global deletion of the segment that contained the *Ankrd1* proximal promoter through exon 2.

wound. Each site was covered with a Tegaderm (3M, St. Paul, MN) dressing to prevent dehydration and infection, and each mouse was fitted with a fabric sleeve (1.6-cm Surgitube; Western Medical Ltd, Tenafly, NJ) to prevent the wound site from being disturbed. Animals were maintained in cages with a 37°C warming pad covering 50% of the cage bottom during a recovery period of 4 to 6 hours, after which time cages were returned to the animal facility. Each subject received 1 mL i.p. of warm 0.9% sodium chloride for 3 days to avoid dehydration. The dressing was removed at day 7. Wound dimensions were measured with an electronic digital caliper (15-cm; Harbor Freight Tools, Camarillo, CA) on alternate days, beginning at day 7 until healing was complete.

An ischemic skin flap was generated on the dorsum by making 1.5 × 2.0-cm skin flaps with a rostral pedicle and underlying the full flap with a 0.13-mm thick silicone sheet (Invotec International, Jacksonville, FL) that extended s.c. 0.25 cm beyond the flap boundaries.[10] The silicone sheet was sutured to the internal fascia, and the flap margins were sutured to close the incisions. This paradigm effectively prevented subdermal blood vessel infiltration into the flap from anywhere other than the pedicle, generating a graded, proximodistal ischemia. Mice were euthanized at indicated time points, and the flaps were removed, cut either transversely or longitudinally, and prepared for histological analysis.

## Transduction of ad*Ankrd1*-GFP into Ischemic Skin Flaps

Fibrin clots containing virus were generated by mixing 10 mg/mL fibrinogen (Sigma-Aldrich, St. Louis, MO), 100 U/mL thrombin (Sigma-Aldrich), and adenovirus expressing either luciferase plus green fluorescent protein (GFP; ad*Luc*-GFP; control) or ANKRD1 plus GFP (ad*Ankrd1*-GFP)[1] so that the final concentrations in the vehicle were 5 mg/mL fibrinogen, 20 U/mL thrombin, and $2 \times 10^{10}$ plaque-forming units of adenovirus per flap. Control flaps were treated with an equivalent dose of ad*Luc*-GFP in fibrin vehicle. Sterile saline was added to adjust the volume of the solutions as needed. Virus (300 μL in fibrin vehicle) was injected between the skin and the silicone sheet of each closed flap.

## Histological Analysis

Mice were euthanized by $CO_2$ asphyxiation at the times indicated later. The wounds plus surrounding skin were excised and fixed in neutral-buffered formalin overnight at 4°C, embedded in paraffin, divided into sections, stained with hematoxylin and eosin or Masson's trichrome green stain, and imaged (Olympus BX50 microscope, DP71 camera, and Software CellSens Standard 1.6; Olympus Corporation, Center Valley, PA). Digital images of each excisional wound were used to determine the distance

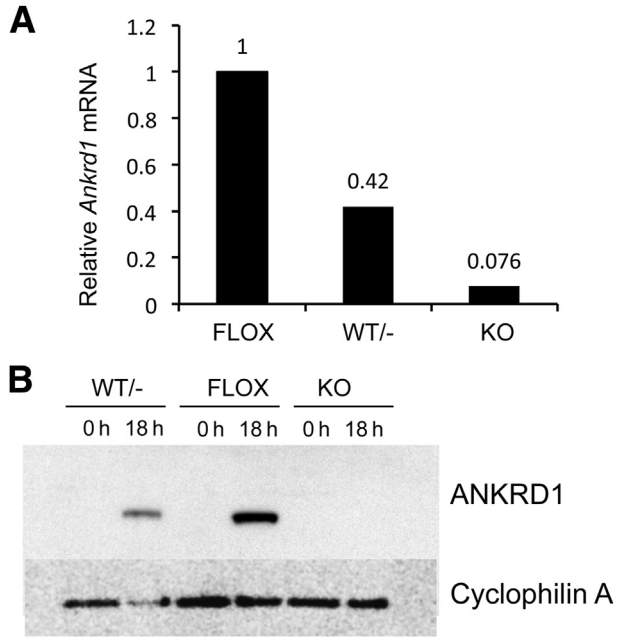


**Figure 2** Partial or complete deletion of Ankrd1 mRNA and protein. Two 6-mm skin biopsy specimens were taken from the dorsum of FLOX, wild-type (WT)/−, and knockout (KO) mice for RNA and protein analysis. **A:** *Ankrd1* mRNA is reduced to 42% of the FLOX levels in hemizygous mice and is essentially undetectable in KO mice. **B:** Western blot analysis of ANKRD1 protein is difficult to detect in uninjured (0 hours) skin of all three genotypes[1] but is sharply induced at 18 hours after wounding in both WT/− and FLOX mice. Induction in hemizygous mice is approximately 50% that of the FLOX mice, whereas no ANKRD1 is detected in KO mice. Cyclophilin A was used as a loading control. h, hours.

between the edges of the panniculus carnosus as a measure of original wound gap using ImageJ software. Digital images of the wounds were also used to measure the granulation tissue thickness and cross-sectional area and the extent of ischemic flap necrosis with a 4× objective.

## Cells

Mouse dermal fibroblasts were isolated from FLOX and KO neonatal skin, as previously described.[11] Early-passage populations of the isolated skin fibroblasts were immortalized with a simian virus (SV)40 large T-antigen plasmid.[12] Briefly, 100-mm dishes of primary cells at 80% to 90% confluence were transfected with 8 μg of plasmid using Lipofectamine (Life Technologies, Grand Island, NY) overnight at 37°C in 5% $CO_2$, after which the transfection reagent was removed and growth medium was added.[12] Both primary and immortalized cells were grown in Dulbecco's modified Eagle's medium (DMEM) containing 10% fetal bovine serum (FBS), 100 U/mL penicillin-streptomycin (P/S), 1% antibiotic-antimycotic (AA), and 2 mmol/L L-glutamine.

## Migration Assay

Of a 12-well tissue culture plate, 4 wells were coated with extracellular matrix (ECM) molecules by incubation in a tissue culture hood at room temperature. In each plate, two wells were coated with collagen (rat tail type I; 100 μg/mL; BD Biosciences, Bedford, MA) and two wells were coated with fibronectin (10 μg/mL; Santa Cruz Biotechnology, Santa Cruz, CA), both in phosphate-buffered saline (PBS). ECM solutions were removed after 2 hours, and the wells were washed with sterile PBS and incubated with serum-free DMEM at 37°C in 5% $CO_2$. FLOX and KO fibroblasts at 80% confluence were trypsinized from flasks and counted and diluted to a concentration of $6 \times 10^5$ cells/mL, a concentration that permitted cells to reach confluence 24 hours after plating. ECM-coated cell culture plates were secured onto a magnetic array that aligned magnets in the center of each of four coated wells. The media were removed from the four coated wells, 500 μL of fresh growth medium was added, and sterile, magnetically adherent stencils[13] (MAtS) (Supplemental Figure S1) were placed in the center of each well. Cell suspensions (500 μL each) were equally distributed around the MAtS, one cell type per ECM, and the plates were incubated for 24 hours to allow cells to attach and reach confluence. Plates were removed from the magnetic array,

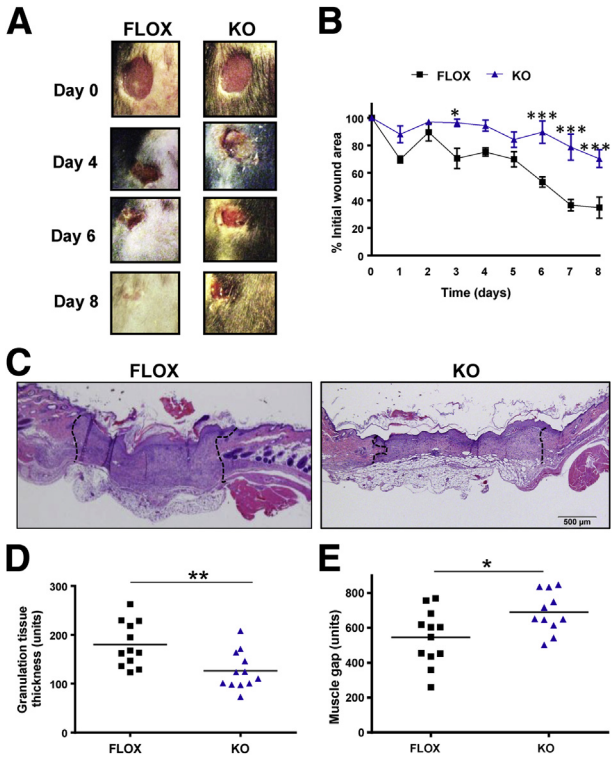


**Figure 3** Delayed excisional wound closure in *Ankrd1*$^{-/-}$ mice. **A:** Gross images of wounds at days 0, 4, 6, and 8 after biopsy show larger wound areas for knockout (KO) mice compared to FLOX mice. **B:** The relative open wound area decreases more rapidly in FLOX mice than KO mice. **C:** Hematoxylin and eosin staining in representative FLOX and KO wounds shows wider and thinner granulation tissue (dotted lines) in KO wounds. **D:** Granulation tissue thickness is significantly reduced in KO wounds compared to wounds in FLOX mice. **E:** A larger wound gap between the cut edges of the panniculus carnosus (muscle gap) is measured in KO compared to FLOX wounds. $n = 12$ (**D** and **E**). $^*P \leq 0.05$, $^{***}P < 0.001$, one-way analysis of variance (**B**); $^*P \leq 0.05$, $^{**}P < 0.01$, Student's *t*-test (**D** and **E**).

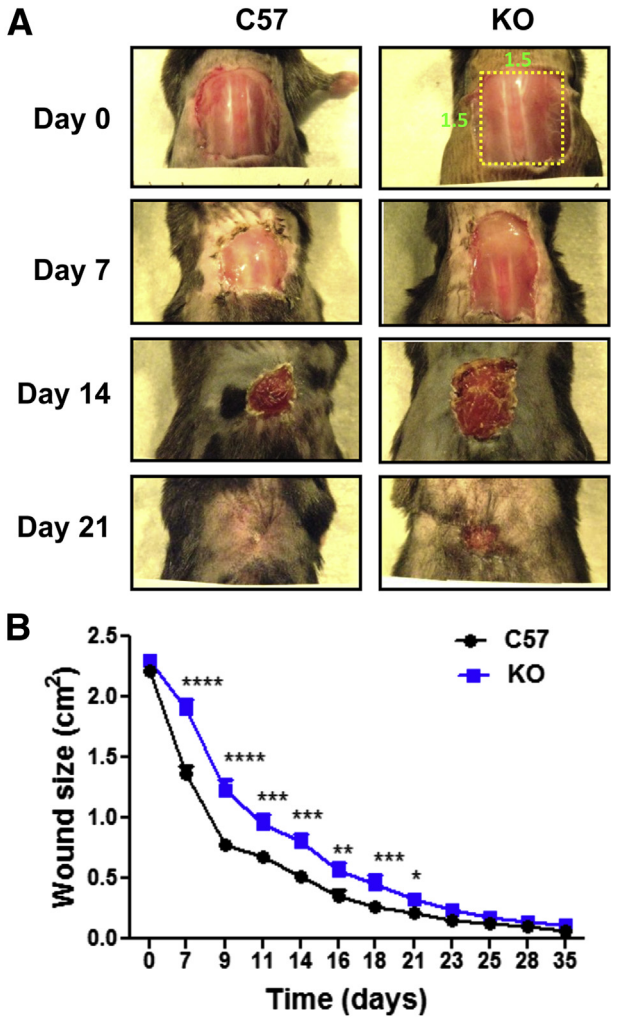


**Figure 4** Protracted delay of large wound closure in the *Ankrd1*$^{-/-}$ mouse. **A:** The 2.25-cm$^2$ wounds close much more slowly than small excisions, yielding a protracted healing response in the knockout (KO) mouse compared to a cohort of equivalent age and size C57Bl/6J controls. **B:** Wound dimensions consistently decrease in the KO strain. Statistically significant differences (multiple *t*-tests) were present up to 21 days. $^*P < 0.05$, $^{**}P < 0.01$, $^{***}P < 0.001$, and $^{****}P < 0.0001$.

and the medium was carefully aspirated, to remove floating cells, and replaced with fresh growth medium. The MAtS were carefully removed to leave a cell-free, undisturbed, four-arm, ECM-coated area in the center of each well. The cell-free wells were filled with warm PBS to help prevent drying of open plates, and the plate was placed in a humidified stage incubator (Bioscience Tools, San Diego, CA) infused with 5% $CO_2$, attached to a Zeiss Axiovert 200M microscope (Carl Zeiss Microscopy LLC, Thornwood, NY) with an automated stage driven by the Ludl Mac 2000 driver module (Ludl Electronic Products Ltd., Hawthorne, NY). Images were acquired every 10 minutes for 5 hours with a Tucsen 3.3 MP cooled charge-coupled device digital microscope camera (OnFocus Laboratories, Lilburn, GA) using a 10× objective. ImagePro Plus 3D with StagePro software version 6.0 (Media Cybernetics Inc., Bethesda, MD) for time-lapse image acquisition was used to acquire and process images. Data analysis to determine percentage of total pixels that were not covered (percentage open area) was done using TScratch software version 1.0 for Windows without Matlab Compiler Runtime (Swiss Federal Institute of Technology in Zürich, Zürich, Switzerland).[14]

## Collagen Gel Contraction

Three-dimensional collagen lattices were prepared as previously described.[15] Briefly, type I rat tail collagen (BD Biosciences, San Jose, CA) was diluted with 20 mmol/L acetic acid to 3 mg/mL. Primary or immortalized skin fibroblasts isolated from neonatal FLOX and KO mice were cultured in DMEM (10% FBS, 1% AA, and 1% P/S), trypsinized, and counted. Collagen (200 μL) neutralized to pH 7.0 with 1N sodium hydroxide was loaded into each well of a 24-well plate. Cells ($1.5 \times 10^5$) were suspended in 400 μL of DMEM (10% FBS, 1% AA, and 1% P/S) and added to the wells containing 200 μL of collagen solution to yield a final concentration of 1 mg/mL. The gels were then incubated at 5% $CO_2$ and 37°C for 30 minutes to allow the collagen to polymerize. After collagen polymerization, 500 μL of DMEM (10% FBS, 1% AA, and 1% P/S) was added to each well. By using a sterile spatula, each gel was mechanically released from the wall and bottom of the wells. Collagen lattices were imaged (GelLogic200

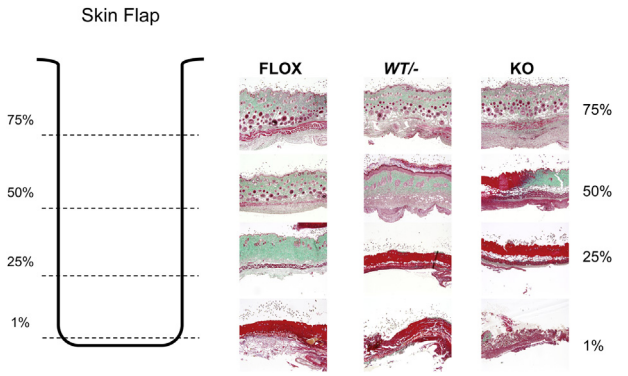


**Figure 5** Necrosis of ischemic skin flaps correlates with *Ankrd1* zygosity. Diagram depicts the sectioning pattern of the ischemic dorsal skin flap. After euthanasia at 12 days, the flaps were excised, cut horizontally into four 4-mm strips (dashed lines) to represent the tissue response as a function of distance from the (cranial) base of the flap, and embedded with the caudal edge of each segment at the paraffin block face. Histological sections, 4× objective: The base of flaps, irrespective of genotype, shows an intact epidermis, a pale green dermis penetrated by numerous hair follicles, s.c. fat, and a deep red panniculus carnosus. At 50% of flap length, hemizygous flaps show a hypertrophic epidermis, immature follicular structures, and a granular dermal response, suggesting incomplete repair. Knockout (KO) flaps show a transition from intact, condensed dermal collagen to frank necrosis (bright red with trichrome staining). By 75% of the flap length, FLOX tissues also undergo signs of deterioration, whereas hemizygous and KO tissues are highly necrotic. Frank necrosis is present at the tip of the flaps, although tissue disintegration is more prominent in the KO animals. Necrosis at the distal end of the ischemic dorsal skin flaps of FLOX mice is minimal, <10% of flap length. WT/$^-$ mice showed approximately 25% to 50% necrosis, whereas 50% to 75% of the flap on *KO* mice became necrotic. Similar results were obtained in three separate experiments.

Imaging System, Molecular Imaging System version 7.1; Carestream Health, Inc., Woodbridge, CT) every 24 hours, and lattice area was analyzed using the Molecular Imaging software (Carestream Health, Inc.). Reduction in lattice area due to contraction was determined at daily intervals up to 7 days.

### Adenovirus Infection/Reconstitution

FLOX and KO immortalized skin fibroblasts were infected with either ad*Ankrd1*-GFP or ad*Luc*-GFP as a control, at a multiplicity of infection of 100. Cells were harvested 48 hours after infection, and used for collagen gel contraction assays or protein isolation.

### Protein Extraction

Whole cell extracts were prepared in radioimmunoprecipitation assay lysis buffer (Sigma-Aldrich, St. Louis, MO) containing a protease inhibitor cocktail (Complete Mini Protease Inhibitor Tablets; Roche, Mannheim, Germany), followed by sonication at 4°C using a Branson 250 Sonifier (Emerson Industrial Automation, Danbury, CT) with a water bath cup horn attachment. Protein concentration in cleared lysates was determined by BCA protein assay kit (Thermo-Scientific, Rockford, IL), and lysates were stored at −80°C.

### Western Blot Analysis

Aliquots containing 30 μg protein from cell extracts were separated by 10% polyacrylamide SDS-PAGE and transferred to a polyvinylidene difluoride membrane (Immobilon; Millipore, Billerica, MA) using the NuPage (Life Technologies, Carlsbad, CA) blotting apparatus, following the manufacturer's protocol. After blocking with a solution of 10 mmol/L Tris-HCl, pH 8, 150 mmol/L NaCl, 0.05% Tween 20, and 5% milk powder, the membrane was incubated with anti-ANKRD1 antibody (1:2000) and anti-cyclophilin (1:20,000; BML-SA296; Enzo, Farmingdale, NY) at 4°C overnight, followed by incubation with anti-rabbit IgG (C2609; Santa Cruz Biotechnology) at room temperature for 30 minutes. The membrane was washed and incubated with Western Lightning Plus Enhanced Chemiluminescent Reagent (Perkin Elmer, Waltham, MA), and protein bands were visualized and quantified using a Kodak Image Station 4000 MM Pro with Kodak MI software version 5.3.3.17476 (Standard Editon; Carestream Health, Inc.). For the virus reconstitution studies, protein was isolated from cells 48 hours after infection.

### RNA Preparation and Analysis

RNA was isolated using the Illustra RNAspin Mini Isolation Kit (GE Healthcare, Piscataway, NJ), according to manufacturer's instructions. RNA concentration was determined spectrophotometrically (Nanodrop; Thermo Scientific, Wilmington, DE), and samples were stored at −80°C.

TaqMan real-time quantitative PCR for *Ankrd1*, *Ankrd2*, and *Ankrd23* (see probe and primer sequences below) and cyclophilin (Applied Biosystems, Foster City, CA), as the housekeeping control, was performed on 50 ng reverse-transcribed RNA with the following primers and probes: *Ankrd1*, 5′-AGACTCCTTCAGCCAACATGATG-3′ (forward), 5′-CTCTCCATCTCTGAAATCCTCAGG-3′ (reverse), and 5′-CCCCTGCCTCCCCATTGCCATTCT-3′ (probe); *Ankrd2*, 5′-GCAGTGGAGGGGAAAATGAAAG-3′ (forward), 5′-CTGTCCGACGGAACTCATCAC-3′ (reverse), and 5′-TCCGCTGAACCTCCQTCCGCCA-3′ (probe); and *Ankrd23*, 5′-ACTGCCTAGAGCACCTTATCG-3′ (forward), 5′-GGAAGCCACATTCTTCACACC-3′ (reverse), and 5′-GCCCACATCAACGCACAGGATAAG-3′ (probe).

### Phalloidin Staining

Collagen lattices were fixed in 4% paraformaldehyde in phosphate buffer after 3 days of culture. Gels were stained following the manufacturer's instructions. Briefly, fixed collagen gels were treated with 0.1% Triton X-100 (Sigma-Aldrich) in PBS for 5 minutes and washed twice with PBS. To reduce nonspecific staining, 1% bovine serum albumin in PBS was added to the gels for 30 minutes before staining with rhodamine phalloidin (Invitrogen, Carlsbad, CA) and SYTOX green nucleic acid staining (Invitrogen). SYTOX green nucleic acid stain (1 μmol/L) and 12.5 μL of rhodamine phalloidin were diluted in 500 μL PBS per well and incubated with the gels for 30 minutes at room temperature. Gels were washed twice with PBS, followed by confocal analysis under ×20 magnification using the Perkin Elmer Opera QEHS Automated Confocal Microscopy System (PerkinElmer, Waltham, MA) at the Vanderbilt Institute for Integrative Biosystems Research and Education Core Facility. Confocal images were analyzed using Columbus Software version 3.2 (PerkinElmer).

## Results

### *In Vivo* Analysis of *Ankrd1* Deletion

To analyze the effects of *Ankrd1* deletion on wound healing, we placed loxP sites 600 bp upstream of the *Ankrd1* proximal promoter and in intron 2, thereby excising the transcription start site and exon 1 and 2 coding sequences (Figure 1A). This design ensured that *Ankrd1* could, in future studies, be selectively deleted in any tissue that expressed *cre*-recombinase. To achieve global deletion of the protein, *Sox2* promoter-driven, *cre*-recombinase–expressing, C57Bl/6J mice were bred to FLOX mice. Mixed background FLOX, *WT/−*, and KO adult mice were evaluated. All litters had a normal numbers of pups, and genotyping confirmed that each genotype was born at the expected allelic distribution with no obvious effects on development, growth, or reproduction as a result of either the insertion of the *loxP* sites or the deletion of *Ankrd1*, suggesting that *Ankrd1* is expendable under normal physiological conditions in mixed background mice. However, backcrossing for

eight generations into the pure inbred C57Bl/6J strain resulted in a growth-diminishing effect of *Ankrd1* deletion that was observed in the neonate and carried through to the adult (Supplemental Figure S2).

We confirmed the *Ankrd1* deletion by mRNA analysis in skin. Because *Ankrd1* expression is low in normal skin, but sharply and strongly induced after wounding, we generated full-thickness, dorsal excisional wounds in FLOX, *WT/−*, and KO adult mice. Tissue was harvested 18 hours after injury for mRNA and protein analysis. *WT/−* wound tissue had >50% reduction of *Ankrd1* mRNA, and transcripts were essentially undetectable in KO tissue (Figure 2A). Similarly, the ANKRD1 protein content of FLOX wound tissue was strongly amplified over that in intact (0 hours) skin, significantly diminished in *WT/−* wound tissue, and undetectable in wounds of KO mice (Figure 2B). Wound contraction in all three genotypes was similar at 18 hours, although there was a mild impairment in wound contraction in mice with deletion of either one or both *Ankrd1* alleles (Supplemental Figure S3). These data confirmed the complete deletion of *Ankrd1* mRNA and protein expression in skin of KO mice and showed that there was no compensatory overexpression from the WT allele in the *WT/−* mouse.

Because we saw no dramatic effects of *Ankrd1* deletion on development or viability, effects on organ development were studied. Organ weights, expressed as a percentage of body weight, of the spleen, liver, kidney, brain, and skeletal muscle from FLOX, *WT/−*, and KO adult male and female mice showed no differences (Supplemental Figure S4). However, the weight of the cardiac ventricles relative to body weight was moderately increased in female mice with a single *Ankrd1* allele, and relative ventricular weight in both sexes increased significantly with the deletion of both alleles (Supplemental Figure S4).

To evaluate histopathological changes that might occur with aging after *Ankrd1* deletion, young (5 to 6 months old) and aged (>1 year) adult male and female, FLOX and KO mice were examined in the Vanderbilt Comparative Pathology Core. Gross visual examination by a veterinary pathologist found no abnormalities in any tissues. Microscopic examination of hematoxylin and eosin–stained sections from all major organ systems also revealed no abnormalities.

### Ankrd2 and Ankrd23 Expression Does Not Compensate for the Loss of Ankrd1

The three members of the MARP family are functionally redundant, at least in skeletal muscle.[6] To investigate possible compensation for *Ankrd1* deletion by one or both of the other MARPs, skin, heart, and skeletal muscle samples were collected from FLOX and KO mice for quantification of *Ankrd2* and *Ankrd23* mRNA. There was no difference in *Ankrd23* mRNA levels in any of the three tissues. *Ankrd2* mRNA, the primary MARP in skeletal muscle, decreased in both skeletal muscle tissue and skin from KO mice (Supplemental Figure S5). This response was consistent with evidence for an involvement of ANKRD1 in MyoD-dependent transcription of *Ankrd2*.[16] In summary, these data showed that neither *Ankrd2* nor *Ankrd23* compensated, at the transcriptional level, for the loss of *Ankrd1*.

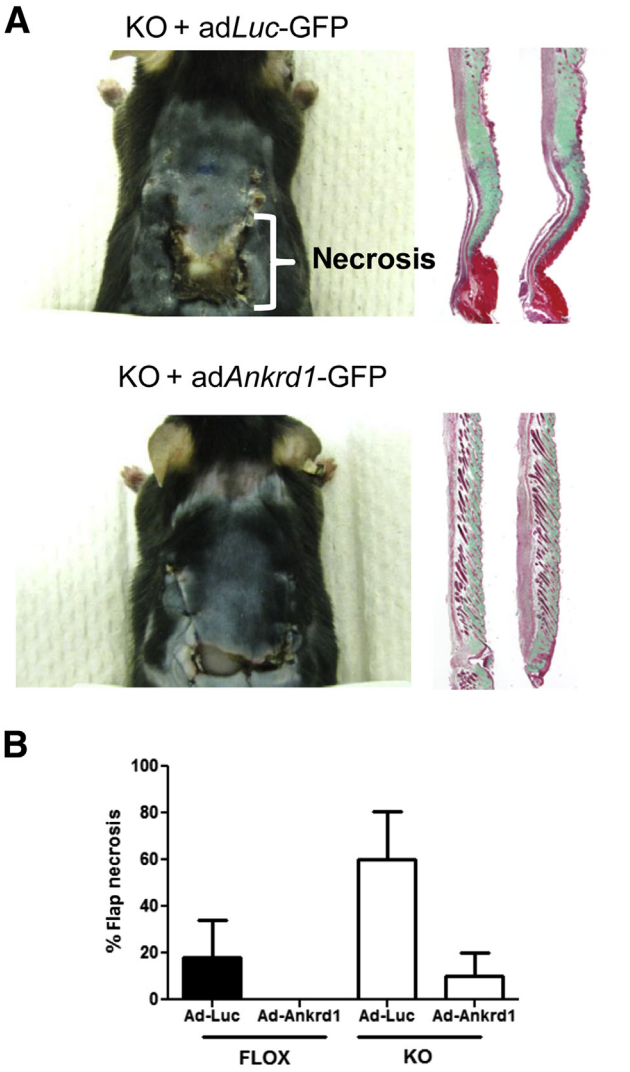


**Figure 6** Adenoviral ANKRD1 overexpression rescues the necrotic phenotype in ischemic *Ankrd1*$^{-/-}$ wounds. **A:** Ischemic flaps in knockout (KO) mice were underlain with fibrin clots containing either adenoviral ad*Luc*-GFP or ad*Ankrd1*-GFP before flap suturing. Mice were euthanized at 10 days. Flaps that received ad*Luc*-GFP have a high percentage of necrosis by day 10, as illustrated in the gross image and in the trichrome green-stained, longitudinal sections. Abnormal dermal architecture and lack of hair follicles are also evident. Flaps treated with an ad*Ankrd1*-GFP vector develop little to no necrosis, dermal alteration, or follicular destruction. **B:** Quantitative analysis of the extent of necrosis in both FLOX and KO mice shows the far greater necrotic response in the KO mouse and the capacity of overexpression of ANKRD1-GFP by adenoviral administration (ad*Ankrd1*-GFP) to reverse the effects of ischemia.

### Deletion of Ankrd1 Produces a Wound Contraction Phenotype

The biological role of ANKRD1 was only partially implicated by the effects of its overexpression[1] and our recent demonstration of the effects of gene deletion on *Mmp13* and *Mmp10* in the KO mouse.[16] On the basis of preliminary observations in 18-hour wounds (Supplemental Figure S3), we analyzed wound contraction in FLOX and KO mice to

the point of near closure. Bilateral, full-thickness, unsplinted excisional wounds (6 mm thick) were made on the dorsum and imaged daily for 8 days (Figure 3A). The wounds of the KO mice contracted more slowly than those of the FLOX mice. Measurements of the wounds showed a particularly significant delay in contraction between 6 and 8 days (Figure 3B). Histomorphometric analysis of KO wound sections revealed both significantly thinner granulation tissue (Figure 3, C and D) and an increased gap between the wound edges, as demarcated by the intact panniculus carnosus of wounds (Figure 3, C and E). However, overall granulation tissue cross-sectional area was similar between the genotypes (Supplemental Figure S6). The change in the shape, rather than the implied volume of granulation tissue, suggested that the delay in closure of KO wounds resulted from decreased contraction and not overall granulation tissue formation. By using this contraction model, epithelialization was unimpeded in the KO group.

Because small excisional wounds contract rapidly, we repeated the analysis with WT C57Bl/6J and eighth-generation C57Bl/6J-backcrossed KO mice of matching age and weight in a second model, a large excisional wound (Figure 4A). The large wound dimensions override the ability of loose murine skin to extend rapidly over the wound, and granulation tissue evolves over several weeks into a dense scar with aligned collagen fibers (data not shown). In this model, KO wound contraction and closure were significantly retarded relative to FLOX mice until at least 21 days after injury (Figure 4B). Wound size remained higher in the KO mice throughout the experiment.

### Reduction or Loss of Ankrd1 Results in Increased Necrosis of Ischemic Skin Flaps

We previously showed that virally mediated overexpression of ANKRD1 in wound models resulted in markedly increased blood vessel development.[1] To study the effect of *Ankrd1* depletion in an ischemic wound model, we generated dorsal skin flaps in the three *Ankrd1* genotypes, with a rostral pedicle that was underlain with a silicone sheet. By 12 days, distinct, progressively more severe degrees of necrosis were evident in the flaps of FLOX, *WT/−*, and KO mice, respectively (Figure 5). In representative transverse sections, trichrome staining showed overt necrosis at only the distal portion of the FLOX flap, with increased collagen density, reduced cellularity, and fewer hair follicles in the distal 25%. The *WT/−* flap showed an intermediate response, with increased necrosis through at least 25% of the flap, reduction of hair follicles, increased collagen condensation, and dermal thickening at 50% of the flap length. This effect was far more exaggerated in the KO flap, with overt necrosis, loss of epidermal appendages, and severe alteration of dermal architecture evident in 50% of the flap. Analysis of several flaps confirmed the progressive extent of ischemic damage with deletion of one or both *Ankrd1* alleles.

To show that the absence of ANKRD1 was central to the necrotic phenotype in the ischemic flap, ANKRD1 was

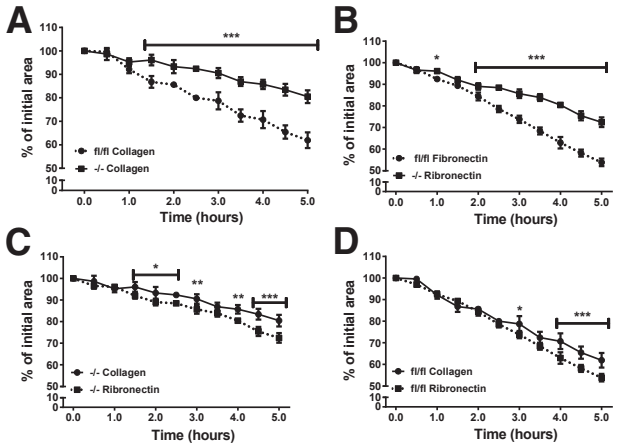


**Figure 7** Deletion of *Ankrd1* retards fibroblast migration on collagen and fibronectin substrates. Migration of FLOX (fl/fl) and knockout (KO; −/−) fibroblasts was studied on fibronectin or collagen-coated surfaces using the magnetically adherent stencils (MAtS) technique to form a gap in the monolayer. **A:** Comparative migration on a collagen substrate. KO fibroblasts (squares: solid line) migrate significantly slower on collagen than FLOX cells (circles: dotted line), with differences seen as early as 1.5 hours. **B:** Comparative migration on a fibronectin substrate. KO fibroblast migration on fibronectin is significantly slower than FLOX fibroblasts at 1.0 hours and more so from 2 to 5 hours. **C:** Relative migration of KO cells on two substrates. KO fibroblasts migrate more rapidly on fibronectin than on collagen. **D:** Relative migration of FLOX fibroblasts. These cells migrate at similar rates on fibronectin and collagen, although significant differences are seen at later time points (two-way analysis of variance with Bonferroni multiple-comparisons test). $*P < 0.05$ (**B**); $***P < 0.001$ (**A** and **B**); $*P < 0.05$ (1.5 to 2.5 hours), $**P < 0.01$ (both 3.0 and 4.0 hours), and $***P < 0.001$ (4.5 to 5.0 hours) (**C**); $*P < 0.05$ (3.0 hours), $***P < 0.001$ (4.0 to 5.0 hours) (**D**).

virally reconstituted in the flaps of KO and FLOX mice. Adenoviral particles that transduced either luciferase plus GFP or ANKRD1 plus GFP were embedded in fibrin clots and placed between the silicone sheet and the skin flap to release viral particles into the overlying flap tissue. Viral expression was confirmed by bioluminescent and fluorescence imaging of mice that were transduced with the ad*Luc*-GFP construct (Supplemental Figure S7). The flaps of KO mice transduced with ad*Luc*-GFP showed the same necrotic phenotype as untransduced KO mice (Figure 6A). In contrast, the mice transduced with ad*Ankrd1*-GFP showed significantly reduced necrosis. Quantification of the effects of both gene deletion and viral treatment in both genotypes is shown in Figure 6B. In flaps of the FLOX mouse treated with the control virus, tissue necrosis was 20%, whereas KO mice showed a threefold increase in tissue damage. In the presence of adenoviral-delivered ANKRD1, FLOX flaps showed little to no necrosis, whereas the necrotic response in the KO animals was reduced by a factor of 6.

## *In Vitro* Analysis of *Ankrd1* Deletion

### Dermal Fibroblasts from KO Mice Have an Altered Phenotype

Because granulation tissue morphological characteristics were differentially affected by *Ankrd1* deletion, dermal fibroblasts were isolated from KO and FLOX mice and

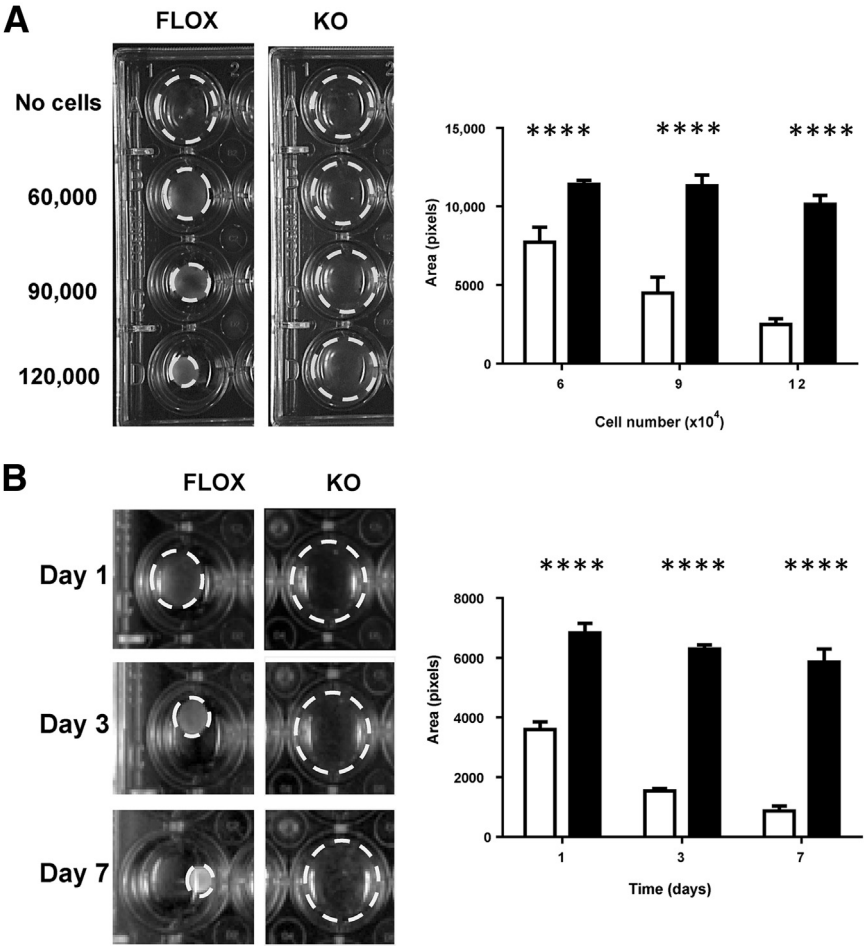


**Figure 8** *Ankrd1*$^{-/-}$ fibroblasts fail to contract collagen gels. **A:** Cell number dependency. Cells ($6 \times 10^4$, $9 \times 10^4$, or $1.2 \times 10^5$ per well) were plated in 1 mg/mL collagen lattices in a 24-well tissue culture plate and were detached after polymerization (**left panel**). After 24 hours, detached lattices (dashed circles) containing FLOX fibroblasts demonstrate increasing collagen contraction in a cell number–dependent manner, whereas no contraction occurs in collagen lattices containing knockout (KO) fibroblasts, regardless of cell number. Quantification of the collagen lattice area. Cell density–dependent collagen lattice contraction at day 1 is significantly different between FLOX (white bars) and KO (black bars) fibroblasts (**right panel**). **B:** Time dependency. Collagen lattices (1 mg/mL) containing $1.5 \times 10^5$ cells per well were formed in 24-well culture plates and detached at 24 hours. Collagen lattices containing FLOX fibroblasts contract over time, whereas KO fibroblast lattices maintain a defective ability to contract up to day 7 (**left panel**). Quantification of collagen gel area over a 7-day interval. FLOX fibroblasts produce rapid, time-dependent contraction, whereas little contraction is observed in KO fibroblasts up to 7 days (**right panel**). ****$P < 0.0001$, Student's *t*-test.

immortalized with the SV40 large T antigen. Experiments were performed with cells between passages 2 and 10, because all of the cells exhibited morphological changes at a higher passage (Supplemental Figure S8).

Adhesion to and migration on ECM were analyzed using a MAtS assay with both collagen I and fibronectin substrates (as described in *Materials and Methods*). We observed that KO cells took longer than FLOX cells to attach to the collagen matrix, but both fibroblast genotypes were stably attached before stencil removal, which initiated cell migration. Both KO and FLOX cells closed the open area more completely on fibronectin-coated (open area, FLOX versus KO = 54% ± 1.75% versus 72% ± 0.24%) than on collagen-coated (open area, FLOX versus KO = 62% ± 3.36% versus 80% ± 2.71%) substrate (Figure 7, A and B). Both cell types migrated to a significantly lesser extent on collagen than fibronectin ($P < 0.001$ at 5 hours) (Figure 7, C and D), and KO fibroblast migration was significantly slower than FLOX migration on either substrate. In summary, KO fibroblasts had an impaired ability to interact with and to migrate on two common matrix substrates.

### KO Fibroblasts Fail to Contract Collagen Lattices

Wound contraction plays a significant role in closure of dermal wounds in loose-skinned rodents, and wound contraction *in vivo* was markedly affected by the deletion of *Ankrd1*. We used both primary and immortalized KO and FLOX mouse fibroblasts to compare their ability to contract fibroblast-populated collagen lattices (FPCLs). One day after FPCL release from the wall of the tissue culture plate well, there was significant ($P < 0.0001$) contraction, even with the fewest FLOX fibroblasts, but little or no FPCL contraction by KO cells, irrespective of the cell number (Figure 8A). KO fibroblast-populated FPCL failed to significantly contract FPCL, even when incubated for up to a week (Figure 8B) or with increasing serum concentration (Supplemental Figure S9). Similar results were found when using nonimmortalized cells.

Reconstitution of ANKRD1 by viral transduction was used to show that the absence of ANKRD1 was central to the contraction failure phenotype of the KO cells. Western blot analysis showed that transduction with ad*Luc*-GFP had no effect on cellular ANKRD1 levels in KO cells (Figure 9A). Transduction with ad*Ankrd1*-GFP increased ANKRD1 in FLOX cells and reconstituted expression in KO cells (Figure 9A). Amplification of ANKRD1 in FLOX fibroblasts improved their ability to contract the FPCL fibroblasts and increased the rate of contraction in KO cells by a factor of approximately 3 (Figure 9B). Rhodamine-phalloidin staining

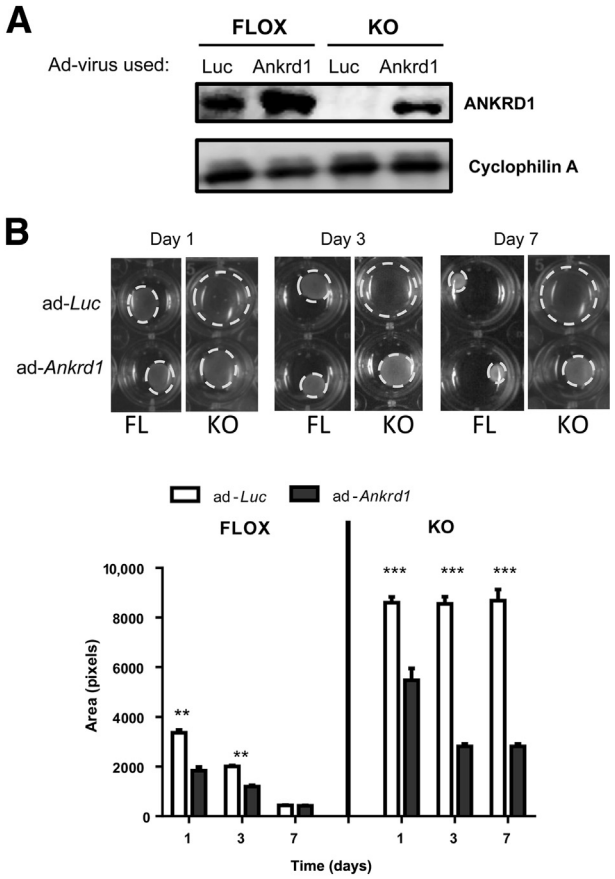


**Figure 9** Reconstitution of ANKRD1 in *Ankrd1*$^{-/-}$ fibroblasts restores their ability to contract collagen lattices. **A:** Western blot analysis of FLOX fibroblasts infected with ad*Luc*—green fluorescent protein (GFP; Luc) and ad*Ankrd1*-GFP (Ankrd1) show overexpression of ANKRD1 after infection with ad*Ankrd1*-GFP. ANKRD1 protein is absent in extracts from knockout (KO) fibroblasts infected with ad*Luc*-GFP but is easily detectable after infection with ad*Ankrd1*-GFP. Cyclophilin A was used as a loading control. **B:** Gel contraction (dashed circles) accelerates by overexpression of ANKRD1 in FLOX fibroblasts at days 1 and 3; reconstitution of ANKRD1 in KO fibroblasts is significantly restored. KO fibroblast contraction at all time points. $^{**}P < 0.01$ (FLOX group), $^{***}P < 0.001$ (KO group), multiple *t*-tests.

of F-actin in FPCL after infection of FLOX fibroblasts with ad*Luc*-GFP revealed an abundant filamentous actin network, whereas there was poor actin assembly or formation of cellular extensions in similarly transduced KO fibroblasts (Figure 10). Adenoviral reconstitution of ANKRD1 in KO fibroblasts under conditions that also promoted gel contraction increased the staining of an F-actin network. These data are consistent with our *in vivo* wound closure studies and suggest that ANKRD1 is necessary for proper interaction of fibroblasts with a collagenous matrix, at least under low tension, *in vivo* and *in vitro*.

## Discussion

Elevated *Ankrd1* expression marks numerous developmental and pathological events, including cardiomyogenesis and neovascularization during tissue repair, and overexpression of *Ankrd1* can enhance healing in several animal wound models.[17,18] Despite the resultant implication that ANKRD1 could be critical to development, we found that global deletion of murine *Ankrd1* yielded ventricular mass increases (in a mixed genetic background), whereas an effect on growth emerged in the pure, inbred C57Bl/6J background. In contrast to the modest developmental effects, the physiological stress of two types of wounding clearly discriminated the *Ankrd1* phenotype. Ischemic injury produced a dramatic defect in skin flap survival that was proportional to gene dosage and was corrected by adenoviral gene delivery. This vascular effect was consistent with our earlier observations on ANKRD1 overexpression in several wound models.[1] *Ankrd1* deletion also retarded excisional wound closure and granulation tissue contraction; furthermore, both the matrix-dependent migration and contractility of KO skin fibroblasts were markedly impaired compared to normal cells. Previous reports of deletion of one or all of the MARPs have detected minor effects.[6,7,19] The present findings in ischemic flaps and excisional wounds are highly consistent with the concept that ANKRD1 abundance becomes a rate-limiting factor when cells and tissues are challenged by injury and stress.

Because of the widespread expression of *Ankrd1* during development and injury, we began an exploration of the role of ANKRD1 by a global deletion of the gene from a FLOX mouse strain using a *Sox2* promoter-driven *cre*-recombinase that is activated in the oocyte. Although gene deletion was readily confirmed in both the hemizygous and homozygous states, the offspring showed no striking pathological conditions

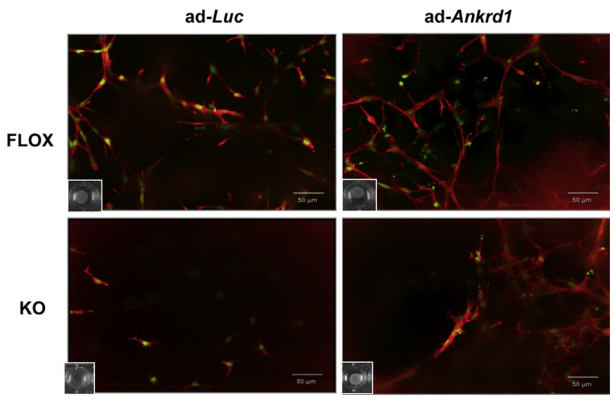


**Figure 10** Actin-rich network assembly after reconstitution of ANKRD1 in *Ankrd1*-deficient fibroblasts. Collagen lattices were loaded with equal numbers of FLOX or knockout (KO) fibroblasts and infected with either adenoviral luciferase—green fluorescent protein (GFP; ad*Luc*-GFP) or ANKRD1-GFP (ad*Ankrd1*-GFP) expression vectors. Cells were stained with phalloidin-red (actin) and SYTOX green (nuclei). Fibrillar actin networks are prominent in collagen gels populated with FLOX fibroblasts infected with ad*Luc*-GFP (ad-*Luc*) and are more abundant after ANKRD1 overexpression with ad*Ankrd1*-GFP (ad-*Ankrd1*). Actin fibers are nearly absent in KO cells treated with ad*Luc*-GFP and markedly increase by ANKRD1 overexpression. **Insets:** The degree of fibroblast-populated collagen lattice contraction, as illustrated in Figure 9. Collaged lattices populated by KO fibroblasts had a much lower cell density because of absent (ad*Luc*-GFP) or reduced (ad*Ankrd1*-GFP) contraction.

and a normal litter size. With continued inbreeding of the original 129 line to a pure C57Bl/6J background, the null offspring showed a mild growth effect. In light of the modest phenotype, we considered the possible compensatory effects of the other two MARP proteins; however, at the level of gene expression, there was no evidence of MARP up-regulation in response to *Ankrd1* deletion. Indeed, there appeared to be a reduced level of *Ankrd2* expression that could be related to the inhibition of MyoD-dependent *Ankrd2* expression after knockdown of *Ankrd1* by siRNA treatment of skeletal muscle.[16] Deletion of all three MARPs provides evidence of skeletal muscle weakness,[6] but the mouse strains in that study showed no developmental abnormalities, as in this report, or, in a more recent report, response to cardiac pressure overload.[7] However, we have recently identified *Ankrd1*-dependent abnormalities in mice after both myocardial infarction and α-adrenergic stimulation (L. Zhong, M. Chiusa, A. Cadar, A. Lin, S.E. Samaras, J.M. Davidson, C.C. Lim, unpublished data).

## Cellular Actions of Ankrd1

The interpretation of the *Ankrd1*-null phenotype is complicated by the multiple roles of ANKRD1. In the sarcomere, ANKRD1 is a titin-associated structural component that, together with myopalladin, calpain protease p94, and calsequestrin, forms a complex that appears to be critical for sarcomere stability of differentiating cardiomyocytes *in vitro*.[3,4,20,21] Reduction of *Ankrd1* mRNA and protein in rat cardiomyocytes by siRNA or doxorubicin leads to sarcomere disintegration and myofibrillar disarray,[20] presumably due to a combination of loss of ANKRD1 from the I-band complex and reduced expression of a range of ANKRD1 transcriptional targets. It has also been suggested that members of the MARP family serve a role in the muscle cell as part of a mechanosensory apparatus, in which MARPs act as shuttles to transport factors, such as Tp53, to the nucleus.[3,21,22] The MARP proteins may also shuttle between cytoplasm and nucleus as part of a stress-related regulatory pathway. We have recently observed that ANKRD1 is involved in the transport of GATA-4 from the sarcomere to the nucleus of the cardiomyocyte (L. Zhong, M. Chiusa, A. Cadar, A. Lin, S.E. Samaras, J.M. Davidson, C.C. Lim, unpublished data).

On the basis of many foregoing studies, depletion of ANKRD1 could be expected to affect both cytoplasmic and nuclear processes. Several studies have suggested that a key role of sarcomeric MARPs is mechanotransduction that is initiated by transportation of the protein from the cytoplasm to the myocyte nucleus.[3] Desmin is another cytoplasmic partner whose depletion leads to up-regulation of *Ankrd1*.[23] The MARPs are associated with several aspects of transcriptional control in striated muscle, including associations with YB-1,[18] Tp53,[16,21] and nucleolin.[16] Early developmental studies showed that the high-level expression of *Ankrd1* was associated with down-regulation of myocyte proteins by association with YB-1. We have recently suggested, on the basis of knockout, knockdown, and overexpression studies in skin fibroblasts, that the association of ANKRD1 with nucleolin leads to the down-regulation of AP-1–stimulated *Mmp13* and *Mmp10* expression.[16]

## The MARP Proteins and Stress

Physiological and pathological stresses affect both expression levels and cellular distribution of the MARPs in striated muscle.[3] Stretch and contraction of striated muscle induce MARP expression as well as increase protein localization in both the I-band and the nucleus. However, some differences have been reported for the individual MARPs between fetal and adult, skeletal and cardiac muscle. Elevated *Ankrd1* expression in humans is widely associated with both hypertrophic and dilated cardiomyopathies,[22,24–26] and ANKRD1 protein and mRNA levels frequently increase in patients with end-stage heart failure.[27,28] Mutations in *Ankrd1* that impair association with the putative mechanosensing complex in the sarcomere have been found in patients with heritable hypertrophic and dilated cardiomyopathies.[4] These mutations were also observed to cause altered muscle-specific gene expression. Although there is less known about ANKRD2 function in the heart, its ability to interact with similar transcriptional regulators as ANKRD1 and to alter muscle-specific protein expression suggests that its dysregulation is also important in cardiac disease.[16]

Alterations in MARP expression in nonmuscle tissue under stress have also been widely observed. Increased ANKRD1 expression in renal podocytes was associated with severity of proteinuria in patients with lupus nephritis[29] and with cisplatin resistance in ovarian cancer chemotherapy.[30] Gene expression profiling after crush injury of peripheral and central dorsal root ganglion neurons suggested that the expression of ANKRD1 might contribute to nerve regeneration.[31]

## Impaired Wound and Collagen Contraction in the Absence of Ankrd1

Confirming initial observations, we documented reduced contraction and healing in unsplinted excisional wounds of KO mice up to 8 days. Granulation tissue thickness was also significantly reduced in these excisional wounds, although the apparent volume of granulation tissue was similar in both FLOX and somewhat growth-retarded KO mice. A larger, more restrained wound model that compared contraction in weight-matched KO and WT C57Bl/6J mice showed highly significant retardation of wound contraction up to at least 3 weeks.

Although the present report evaluates the effects of global *Ankrd1* deletion, the defect in contraction of the wound margins and granulation tissue was certainly consistent with the inefficiency of KO skin fibroblast migration on matrix-coated substrates and the inability of these null cells to contract a FPCL, a model that is often considered an *in vitro* analogue of (compliant) granulation tissue. Inhibition of

contraction was also observed with aortic vascular smooth muscle cells (unpublished data).

Collagen degradation can influence FPCL contraction.[32] We recently reported that KO fibroblasts strongly up-regulate both *Mmp10* and *Mmp13* expression *in vitro* and *Mmp13* expression *in vivo*.[16] Matrix metalloproteinase (MMP) overexpression was even more strongly induced in both anchored and released FPCL (unpublished data), a response that has been reported to involve an integrin-dependent pathway.[33] In contrast to the reported stimulation of FPCL contraction by virally induced overexpression of human MMP-13[34] or by age-related fibroblast overexpression of rat MMP-2 and MMP-9,[35] elevated *Mmp10* and *Mmp13* gene expression in the KO fibroblast appeared to have no accelerating effect on FPCL reorganization. There may be a defect in the synthesis, secretion, activation, or activity of these metalloproteinases. It is also possible that MMP-10 and MMP-13 activities are concentrated at the cell surface of KO cells, thereby preventing interactions of KO cells with their pericellular environment or, alternatively, that binding and response to ECM is affected by deletion of *Ankrd1*. Further studies will be needed to localize and to determine the relative activities of MMPs and ECM receptors *in vivo* and *in vitro* and to establish the effects of MMP inhibition.

### Necrotic Phenotype in the Absence of Ankrd1

The more dramatic phenotype of the KO mouse was the extent of necrosis in a pedicled flap. The null animals showed extensive flap necrosis, and the haploinsufficient animals confirmed a gene dosage effect. This outcome, particularly in light of rescue by overexpression of adenoviral *Ankrd1*, was consistent with our earlier report on the capacity of adenoviral delivery of *Ankrd1* to enhance neovascularization in several wound models.[1] The susceptibility to vascular insufficiency may also be related to the initial identification of ANKRD1 as a protein prominently expressed in cytokine-stimulated vascular endothelial cells[36] and subsequently localized in vascular smooth muscle cells.[37–39] ANKRD1 has been reported to augment Tp53-stimulated MyoD promoter activity in skeletal muscle cells, whereas Tp53 can augment *Ankrd1* transcription, suggesting a potential positive feedback loop.[21] There is also the potential that overexpression of MMP-10 and MMP-13 is occurring in the KO vasculature as well, exerting an effect on initiation or maturation of stable vasculature. Many forms of stress and injury induce ANKRD1 expression,[5,16,31,40] and MARP proteins may wield more generally protective roles in cells under ischemic stress.[3,41,42] Selective deletion of *Ankrd1* in vascular cells will certainly help to address the vascular aspects of the *Ankrd1*-null phenotype.

The significant effect of *Ankrd1* deletion on wound contraction, together with the dramatic inability of *Ankrd1*-null fibroblasts to contract an ECM equivalent, suggests that ANKRD1 may function in a pathway that normally transduces cell-matrix interaction into contractile activity, at least in the low-tension environment of the FPCL and, by analogy, granulation tissue. In addition to ANKRD1 association with other components in the classic, sarcomere contractile apparatus, ANKRD1 also binds to desmin,[43] and desmin knockdown has suggested that this filamentous protein may regulate *Ankrd1* expression through an Akt/NF-κB pathway.[23] Equally intriguing are the reports that both *Ankrd1* and *CCN2,* which are strongly induced during injury and repair, are downstream transcriptional targets of a mechanical strain response that is mediated by the YAP/TAZ pathway.[44–47] If cell contraction in the FPCL depends on *Ankrd1* expression, then it may be a rate-limiting mediator of mechanotransduction during wound repair, in which there is disruption of the normal mechanical environment.

## Acknowledgments

We thank the Vanderbilt Transgenic Mouse/ESC Shared Resource and Dr. Ron Emeson (Director at the time the reported mice were developed) for helpful discussions; the Vanderbilt Diabetes Research and Training Center; the Vanderbilt Brain Institute; Roy Zent for providing the Sox2-*cre* mice; Erica Pruett for providing support for the analysis of MARP expression; Vanessa Allwardt and the Vanderbilt Institute for Integrative Biosystems Research and Education Automated Biosystem Core for providing assistance with the confocal microscopy; Will Ashby for helping with the migration studies; and Chee Chew Lim and Susan Opalenik, in particular, for many helpful critical comments.

## Supplemental Data

Supplemental material for this article can be found at *http://dx.doi.org/10.1016/j.ajpath.2014.09.018*.

## References

1. Shi Y, Reitmaier B, Regenbogen J, Slowey RM, Opalenik SR, Wolf E, Goppelt A, Davidson JM: CARP, a cardiac ankyrin repeat protein, is up-regulated during wound healing and induces angiogenesis in experimental granulation tissue. Am J Pathol 2005, 166:303–312
2. Miller MK, Bang ML, Witt CC, Labeit D, Trombitas C, Watanabe K, Granzier H, McElhinny AS, Gregorio CC, Labeit S: The muscle ankyrin repeat proteins: CARP, ankrd2/Arpp and DARP as a family of titin filament-based stress response molecules. J Mol Biol 2003, 333: 951–964
3. Kojic S, Radojkovic D, Faulkner G: Muscle ankyrin repeat proteins: their role in striated muscle function in health and disease. Crit Rev Clin Lab Sci 2011, 48:269–294
4. Mikhailov AT, Torrado M: The enigmatic role of the ankyrin repeat domain 1 gene in heart development and disease. Int J Dev Biol 2008, 52:811–821
5. Samaras SE, Shi Y, Davidson JM: CARP: fishing for novel mechanisms of neovascularization. J Investig Dermatol Symp Proc 2006, 11: 124–131

6. Barash IA, Bang ML, Mathew L, Greaser ML, Chen J, Lieber RL: Structural and regulatory roles of muscle ankyrin repeat protein family in skeletal muscle. Am J Physiol Cell Physiol 2007, 293: C218–C227
7. Bang ML, Gu Y, Dalton ND, Peterson KL, Chien KR, Chen J: The muscle ankyrin repeat proteins CARP, Ankrd2, and DARP are not essential for normal cardiac development and function at basal conditions and in response to pressure overload. PLoS One 2014, 9: e93638
8. Adams DJ, Quail MA, Cox T, van der Weyden L, Gorick BD, Su Q, Chan WI, Davies R, Bonfield JK, Law F, Humphray S, Plumb B, Liu P, Rogers J, Bradley A: A genome-wide, end-sequenced 129Sv BAC library resource for targeting vector construction. Genomics 2005, 86:753–758
9. Hayashi S, Tenzen T, McMahon AP: Maternal inheritance of Cre activity in a Sox2Cre deleter strain. Genesis 2003, 37:51–53
10. Tepper OM, Galiano RD, Capla JM, Kalka C, Gagne PJ, Jacobowitz GR, Levine JP, Gurtner GC: Human endothelial progenitor cells from type II diabetics exhibit impaired proliferation, adhesion, and incorporation into vascular structures. Circulation 2002, 106: 2781–2786
11. Normand J, Karasek MA: A method for the isolation and serial propagation of keratinocytes, endothelial cells, and fibroblasts from a single punch biopsy of human skin. In Vitro Cell Dev Biol Anim 1995, 31:447–455
12. Chang LS, Pan S, Pater MM, Di Mayorca G: Differential requirement for SV40 early genes in immortalization and transformation of primary rat and human embryonic cells. Virology 1985, 146:246–261
13. Ashby WJ, Wikswo JP, Zijlstra A: Magnetically attachable stencils and the non-destructive analysis of the contribution made by the underlying matrix to cell migration. Biomaterials 2012, 33:8189–8203
14. Geback T, Schulz MM, Koumoutsakos P, Detmar M: TScratch: a novel and simple software tool for automated analysis of monolayer wound healing assays. Biotechniques 2009, 46:265–274
15. Ngo P, Ramalingam P, Phillips JA, Furuta GT: Collagen gel contraction assay. Methods Mol Biol 2006, 341:103–109
16. Belgrano A, Rakicevic L, Mittempergher L, Campanaro S, Martinelli VC, Mouly V, Valle G, Kojic S, Faulkner G: Multi-tasking role of the mechanosensing protein Ankrd2 in the signaling network of striated muscle. PLoS One 2011, 6:e25519
17. Kuo H, Chen J, Ruiz-Lozano P, Zou Y, Nemer M, Chien KR: Control of segmental expression of the cardiac-restricted ankyrin repeat protein gene by distinct regulatory pathways in murine cardiogenesis. Development 1999, 126:4223–4234
18. Zou Y, Evans S, Chen J, Kuo HC, Harvey RP, Chien KR: CARP, a cardiac ankyrin repeat protein, is downstream in the Nkx2-5 homeobox gene pathway. Development 1997, 124:793–804
19. Bean C, Verma NK, Yamamoto DL, Chemello F, Cenni V, Filomena MC, Chen J, Bang ML, Lanfranchi G: Ankrd2 is a modulator of NF-kappaB-mediated inflammatory responses during muscle differentiation. Cell Death Dis 2014, 5:e1002
20. Chen B, Zhong L, Roush SF, Pentassuglia L, Peng X, Samaras S, Davidson JM, Sawyer DB, Lim CC: Disruption of a GATA4/Ankrd1 signaling axis in cardiomyocytes leads to sarcomere disarray: implications for anthracycline cardiomyopathy. PLoS One 2012, 7:e35743
21. Kojic S, Nestorovic A, Rakicevic L, Belgrano A, Stankovic M, Divac A, Faulkner G: A novel role for cardiac ankyrin repeat protein Ankrd1/CARP as a co-activator of the p53 tumor suppressor protein. Arch Biochem Biophys 2010, 502:60–67
22. Moulik M, Vatta M, Witt SH, Arola AM, Murphy RT, McKenna WJ, Boriek AM, Oka K, Labeit S, Bowles NE, Arimura T, Kimura A, Towbin JA: ANKRD1, the gene encoding cardiac ankyrin repeat protein, is a novel dilated cardiomyopathy gene. J Am Coll Cardiol 2009, 54:325–333
23. Mohamed JS, Boriek AM: Loss of desmin triggers mechanosensitivity and up-regulation of Ankrd1 expression through Akt-NF-kappaB signaling pathway in smooth muscle cells. FASEB J 2012, 26: 757–765
24. Arimura T, Bos JM, Sato A, Kubo T, Okamoto H, Nishi H, Harada H, Koga Y, Moulik M, Doi YL, Towbin JA, Ackerman MJ, Kimura A: Cardiac ankyrin repeat protein gene (ANKRD1) mutations in hypertrophic cardiomyopathy. J Am Coll Cardiol 2009, 54: 334–342
25. Crocini C, Arimura T, Reischmann S, Eder A, Braren I, Hansen A, Eschenhagen T, Kimura A, Carrier L: Impact of ANKRD1 mutations associated with hypertrophic cardiomyopathy on contraction parameters of engineered heart tissue. Basic Res Cardiol 2013, 108:349
26. Duboscq-Bidot L, Charron P, Ruppert V, Fauchier L, Richter A, Tavazzi L, Arbustini E, Wichter T, Maisch B, Komajda M, Isnard R, Villard E: Mutations in the ANKRD1 gene encoding CARP are responsible for human dilated cardiomyopathy. Eur Heart J 2009, 30: 2128–2136
27. Torrado M, Nespereira B, Bouzamayor Y, Centeno A, Lopez E, Mikhailov AT: Differential atrial versus ventricular ANKRD1 gene expression is oppositely regulated at diastolic heart failure. FEBS Lett 2006, 580:4182–4187
28. Zolk O, Frohme M, Maurer A, Kluxen FW, Hentsch B, Zubakov D, Hoheisel JD, Zucker IH, Pepe S, Eschenhagen T: Cardiac ankyrin repeat protein, a negative regulator of cardiac gene expression, is augmented in human heart failure. Biochem Biophys Res Commun 2002, 293:1377–1382
29. Matsuura K, Uesugi N, Hijiya N, Uchida T, Moriyama M: Upregulated expression of cardiac ankyrin-repeated protein in renal podocytes is associated with proteinuria severity in lupus nephritis. Hum Pathol 2007, 38:410–419
30. Scurr LL, Guminski AD, Chiew YE, Balleine RL, Sharma R, Lei Y, Pryor K, Wain GV, Brand A, Byth K, Kennedy C, Rizos H, Harnett PR, deFazio A: Ankyrin repeat domain 1, ANKRD1, a novel determinant of cisplatin sensitivity expressed in ovarian cancer. Clin Cancer Res 2008, 14:6924–6932
31. Stam FJ, MacGillavry HD, Armstrong NJ, de Gunst MC, Zhang Y, van Kesteren RE, Smit AB, Verhaagen J: Identification of candidate transcriptional modulators involved in successful regeneration after nerve injury. Eur J Neurosci 2007, 25:3629–3637
32. Langholz O, Rockel D, Mauch C, Kozlowska E, Bank I, Krieg T, Eckes B: Collagen and collagenase gene expression in three-dimensional collagen lattices are differentially regulated by alpha 1 beta 1 and alpha 2 beta 1 integrins. J Cell Biol 1995, 131:1903–1915
33. Ravanti L, Heino J, Lopez-Otin C, Kahari VM: Induction of collagenase-3 (MMP-13) expression in human skin fibroblasts by three-dimensional collagen is mediated by p38 mitogen-activated protein kinase. J Biol Chem 1999, 274:2446–2455
34. Toriseva MJ, Ala-aho R, Karvinen J, Baker AH, Marjomaki VS, Heino J, Kahari VM: Collagenase-3 (MMP-13) enhances remodeling of three-dimensional collagen and promotes survival of human skin fibroblasts. J Invest Dermatol 2007, 127:49–59
35. Ballas CB, Davidson JM: Delayed wound healing in aged rats is associated with increased collagen gel remodeling and contraction by skin fibroblasts, not with differences in apoptotic or myofibroblast cell populations. Wound Repair Regen 2001, 9:223–237
36. Chu W, Burns DK, Swerlick RA, Presky DH: Identification and characterization of a novel cytokine-inducible nuclear protein from human endothelial cells. J Biol Chem 1995, 270:10236–10245
37. Boengler K, Pipp F, Fernandez B, Ziegelhoeffer T, Schaper W, Deindl E: Arteriogenesis is associated with an induction of the cardiac ankyrin repeat protein (carp). Cardiovasc Res 2003, 59: 573–581
38. de Waard V, van Achterberg TA, Beauchamp NJ, Pannekoek H, de Vries CJ: Cardiac ankyrin repeat protein (CARP) expression in human and murine atherosclerotic lesions: activin induces CARP in smooth muscle cells. Arterioscler Thromb Vasc Biol 2003, 23: 64–68

39. Kanai H, Tanaka T, Aihara Y, Takeda S, Kawabata M, Miyazono K, Nagai R, Kurabayashi M: Transforming growth factor-beta/Smads signaling induces transcription of the cell type-restricted ankyrin repeat protein CARP gene through CAGA motif in vascular smooth muscle cells. Circ Res 2001, 88:30−36
40. Qin W, Pan J, Bauman WA, Cardozo CP: Differential alterations in gene expression profiles contribute to time-dependent effects of nandrolone to prevent denervation atrophy. BMC Genomics 2010, 11:596
41. Casey WM, Brodie T, Yoon L, Ni H, Jordan HL, Cariello NF: Correlation analysis of gene expression and clinical chemistry to identify biomarkers of skeletal myopathy in mice treated with PPAR agonist GW610742X. Biomarkers 2008, 13:364−376
42. Ghosh AK, Murphy SB, Kishore R, Vaughan DE: Global gene expression profiling in PAI-1 knockout murine heart and kidney: molecular basis of cardiac-selective fibrosis. PLoS One 2013, 8: e63825
43. Witt SH, Labeit D, Granzier H, Labeit S, Witt CC: Dimerization of the cardiac ankyrin protein CARP: implications for MARP titin-based signaling. J Muscle Res Cell Motil 2005, 26:401−408
44. Aragona M, Panciera T, Manfrin A, Giulitti S, Michielin F, Elvassore N, Dupont S, Piccolo S: A mechanical checkpoint controls multicellular growth through YAP/TAZ regulation by actin-processing factors. Cell 2013, 154:1047−1059
45. Dupont S, Morsut L, Aragona M, Enzo E, Giulitti S, Cordenonsi M, Zanconato F, Le Digabel J, Forcato M, Bicciato S, Elvassore N, Piccolo S: Role of YAP/TAZ in mechanotransduction. Nature 2011, 474:179−183
46. Halder G, Dupont S, Piccolo S: Transduction of mechanical and cytoskeletal cues by YAP and TAZ. Nat Rev Mol Cell Biol 2012, 13: 591−600
47. Piccolo S, Cordenonsi M, Dupont S: Molecular pathways: YAP and TAZ take center stage in organ growth and tumorigenesis. Clin Cancer Res 2013, 19:4925−4930